



# Single walled carbon nanotube incorporated Titanium dioxide and Poly (3-hexylthiophene) as electron and hole transport materials for perovskite solar cells

Uthayaraj Siva<sup>a,d</sup>, Thanishaichelvan Murugathas<sup>a</sup>, Shivatharsiny Yohi<sup>b</sup>, Muthukumarasamy Natarajan<sup>c</sup>, Dhayalan Velauthapillai<sup>d,\*</sup>, Punniamorthy Ravirajan<sup>a,\*</sup>

<sup>a</sup> Department of Physics, University of Jaffna, Jaffna 40 000, Sri Lanka

<sup>b</sup> Department of Chemistry, University of Jaffna, Jaffna 40 000, Sri Lanka

<sup>c</sup> Department of Physics, Coimbatore Institute of Technology, Coimbatore, Tamil Nadu 641014, India

<sup>d</sup> Faculty of Engineering and Science, Western Norway University of Applied Sciences, P.O. Box 7030, Bergen, Norway

## ARTICLE INFO

### Article history:

Received 15 May 2020

Received in revised form 15 June 2020

Accepted 16 June 2020

Available online 18 June 2020

### Keywords:

Perovskite

Solar cells

Carbon nanotube

TiO<sub>2</sub>

P3HT

## ABSTRACT

This study focuses on incorporating single wall carbon nanotubes (CNTs) in both electron conducting porous Titanium dioxide (TiO<sub>2</sub>) and the hole conducting Poly(3-hexylthiophene) (P3HT) layers in order to enhance the performance of perovskite solar cells. The CNT was incorporated at TiO<sub>2</sub>/CH<sub>3</sub>NH<sub>3</sub>PbI<sub>x</sub>Cl<sub>3-x</sub> interface by dip coating TiO<sub>2</sub> electrodes with CNT solution prior to deposition of CH<sub>3</sub>NH<sub>3</sub>PbI<sub>x</sub>Cl<sub>3-x</sub> and by blending with P3HT, respectively. Raman spectra and Atomic Force Microscopic (AFM) images confirmed the presence of CNT in TiO<sub>2</sub> electrodes and in P3HT, respectively. Optimized devices with the CNT show overall power conversion efficiencies (PCE) over 14%, under 100 mW/cm<sup>2</sup> illumination with Air Mass 1.5 filter, which is 50% higher than that of the control device which is not having CNT. The enhancement is predominantly due to increase in short circuit current density (J<sub>sc</sub>) and fill factor, which resulted from surface passivation at the interface by CNT.

© 2020 Elsevier B.V. All rights reserved.

## 1. Introduction

Perovskite solar cells (PSCs) have become a research hot-spot due to its low-cost fabrication techniques together with high efficiency [1,2]. It has a perovskite layer sandwiched between an electron and hole transporting layer with transparent conducting oxide and gold thin films as the electrodes. Both electron and hole transporting layers play a vital role in charge transport in these PSCs. Optimizing the charge transport properties in these transporting layers is one of the strategies to improve the PCE of PSCs [3]. In recent years, a few works have been focused on the application of CNT in PSCs due to their outstanding electrical, optical, mechanical, and structural properties [4].

In conventional PSCs, TiO<sub>2</sub> is regarded as one of the best electron extracting and transporting material. It was reported that the charge transfer at the interface was significantly improved after introducing CNT in Electron Transporting Materials (ETM), which effectively increases the electron collection [5]. P3HT is

one of the best studied Hole Transporting Material (HTMs) for PSCs. However, the hole-mobility is the key challenge in enhancing the efficiency of PSCs.

In this study, we focus on enhancing the performance of PSCs by utilizing CNTs (i) at TiO<sub>2</sub>/perovskite interface, (ii) in P3HT HTM, and (iii) in both TiO<sub>2</sub>/perovskite interface and P3HT HTM, and to the best of our knowledge this is the first study reporting all these effects together in PSCs.

## 2. Materials and methods

The device fabrication and characterization techniques of PSCs with and without CNT can be found in the [supporting information](#) (SI) and refs. [6,7].

## 3. Results and discussion

In this study, CNT bundles (IsoNanotubes S-99, NanoIntegris, Canada) which are predominantly p-type semiconductors after sonication [8,9] were incorporated at the TiO<sub>2</sub>/CH<sub>3</sub>NH<sub>3</sub>PbI<sub>x</sub>Cl<sub>3-x</sub> interface and/or P3HT. Fig. 1(a) shows the Raman spectra of bare

\* Corresponding authors.

E-mail addresses: [Dhayalan.Velauthapillai@hvl.no](mailto:Dhayalan.Velauthapillai@hvl.no) (D. Velauthapillai), [pravirajan@univ.jfn.ac.lk](mailto:pravirajan@univ.jfn.ac.lk) (P. Ravirajan).

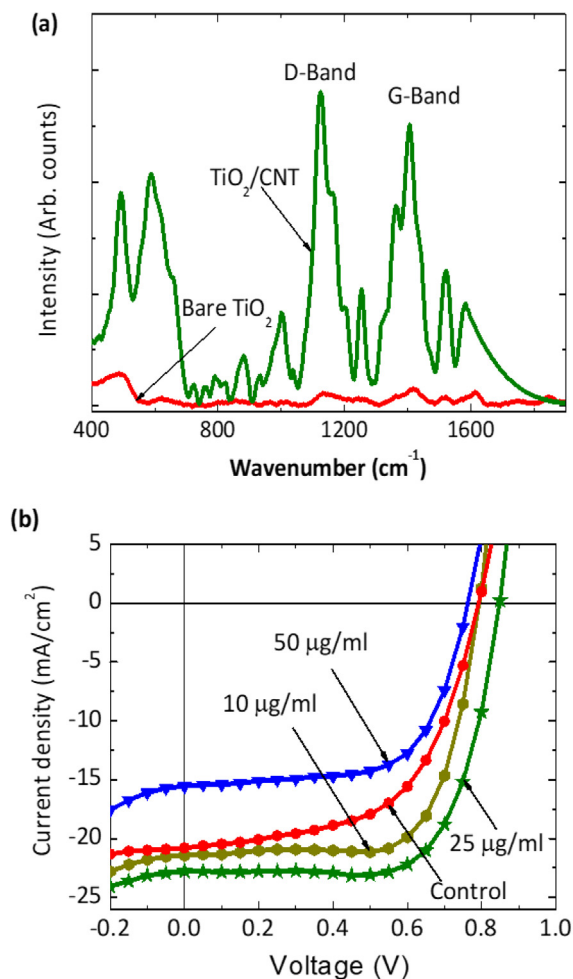


**Fig. 1.** (a) Raman spectra of bare  $\text{TiO}_2$  and CNT incorporated  $\text{TiO}_2$  film, coated on glass plate and (b) J-V characteristics of  $\text{FTO}/\text{TiO}_2/\text{CNT}/\text{CH}_3\text{NH}_3\text{PbI}_{3-x}\text{Cl}_{3-x}/\text{P3HT}/\text{Au}$  devices with different concentration of CNT.

$\text{TiO}_2$  and CNT dip-coated  $\text{TiO}_2$  electrodes, recorded using Raman spectrometer (EZRAMAN, Model: 5B1S-162) with a 532 nm laser. The peaks obtained at the wavenumbers of 1124 and 1407  $\text{cm}^{-1}$  corresponding to D-band and G-band, respectively confirm the presence of CNT [10].

Fig. 1(b) shows the strong influence of CNT at the  $\text{TiO}_2$ /perovskite interface on both fill factor and short circuit current density. Enhancement in the overall performance of PSCs was observed until CNT concentration is increased up to 25  $\mu\text{g}/\text{ml}$ , and this is attributed to the passivation of the electronic defect states at  $\text{TiO}_2/\text{CH}_3\text{NH}_3\text{PbI}_{3-x}\text{Cl}_{3-x}$  interface, this suppresses the recombination, and, hence, improves the FF and  $V_{\text{OC}}$  as reported by Macdonald *et al.*, [11]. The surface passivation achieved by the introduction of optimum CNT results in reduction of series resistance between the layers of the device and this increases the short circuit current density. The conduction band of CNT is present at energetically favorable position near the conduction band of the perovskite forming ideal routes which facilitates the transport of charge carriers towards the FTO electrode, and the nanotubes here act as a bridge between the perovskite and  $\text{TiO}_2$ .

It is observed that the incorporation of CNT increases the absorption of light by  $\text{TiO}_2$ /perovskite electrode (see Fig. S1), and thus, enhances the  $J_{\text{SC}}$  as seen in the J-V data. Introducing CNT on  $\text{TiO}_2$  electrode can change the energy level of the electrode which increases  $V_{\text{OC}}$  as reported by Batmunkh *et al.*, [5]. However, further increase in CNT concentration (50  $\mu\text{g}/\text{ml}$ ) decreases the  $J_{\text{SC}}$  signifi-

cantly due to excess CNT at the interface which obstructs the charge transport.

The effect of CNT in P3HT on the photovoltaic performance of PSCs were also investigated, and the results are presented in Fig. 2(a). The 0.5 wt% of CNT in CNT:P3HT composite was identified as optimum for the fabrication of PSCs, and an enhanced PCE of 12.1% was obtained for this device. CNT provides additional percolation pathways for transportation of electrical charges and only optimal amount of CNT will promote formation of charge percolation pathways, eliminating electrical short-cuts. CNT in P3HT helps to improve hole extraction from the perovskite layer but when the concentration of the CNT in the composite is high, significant charge recombination between the CNTs and perovskite is likely to occur because of the direct contact between them [12].

A clear morphological change is observed in the AFM images obtained for the device with optimum CNT content as indicated in Fig. 2(b) and (c), which can be attributed to the improved polymerization and crystallization of P3HT. Hence, the increased FF can be attributed to the improvement in crystallinity and it is consistent with the previous report [13]. The enhancement in  $J_{\text{SC}}$  and  $V_{\text{OC}}$  can be due to the improvement in hole transport and the mobility in P3HT [14]. Further details of photovoltaic parameters for CNT:P3HT based devices can be found in Table S2, SI.

In the synthesized CNT:P3HT composite, the P3HT molecules penetrate into the CNT network due to the strong  $\pi$ - $\pi$  interactions with dispersed CNTs, and thus, prevent CNT from aggregation. The AFM image shows the formation of almost pin hole free layer which also is responsible for increase in  $J_{\text{SC}}$ . Incorporation of CNT increases the hole conductivity and work function without sacrificing optical transmittance of the HTM, and this results in improvement in the FF and  $J_{\text{SC}}$  of the device.

After the CNT content was optimized in ETM and HTM separately, the PSCs were fabricated with optimized CNT content in both ETM and HTM. The J-V data obtained for champion devices

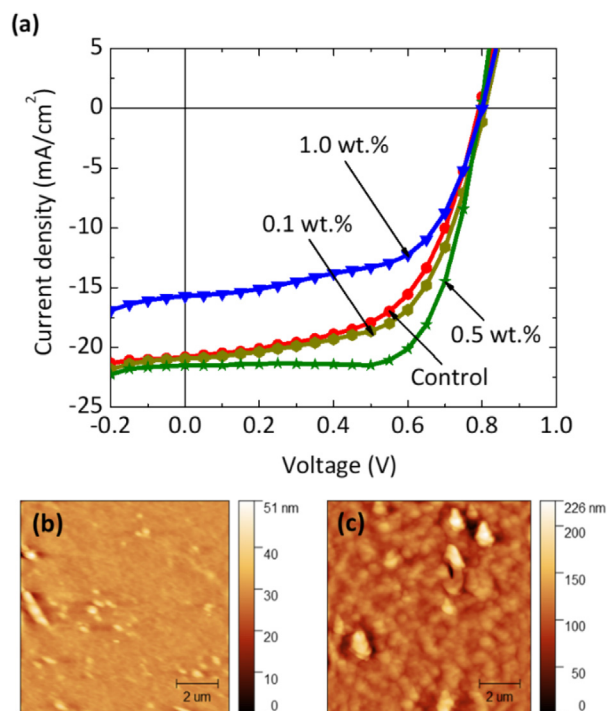


**Fig. 2.** (a) J-V characteristics of  $\text{FTO}/\text{TiO}_2/\text{CH}_3\text{NH}_3\text{PbI}_{3-x}\text{Cl}_{3-x}/\text{CNT:P3HT}/\text{Au}$  devices with different amount of CNT:P3HT composite under illumination and AFM images of (b) pristine and (c) 0.5 wt% CNT doped P3HT film.

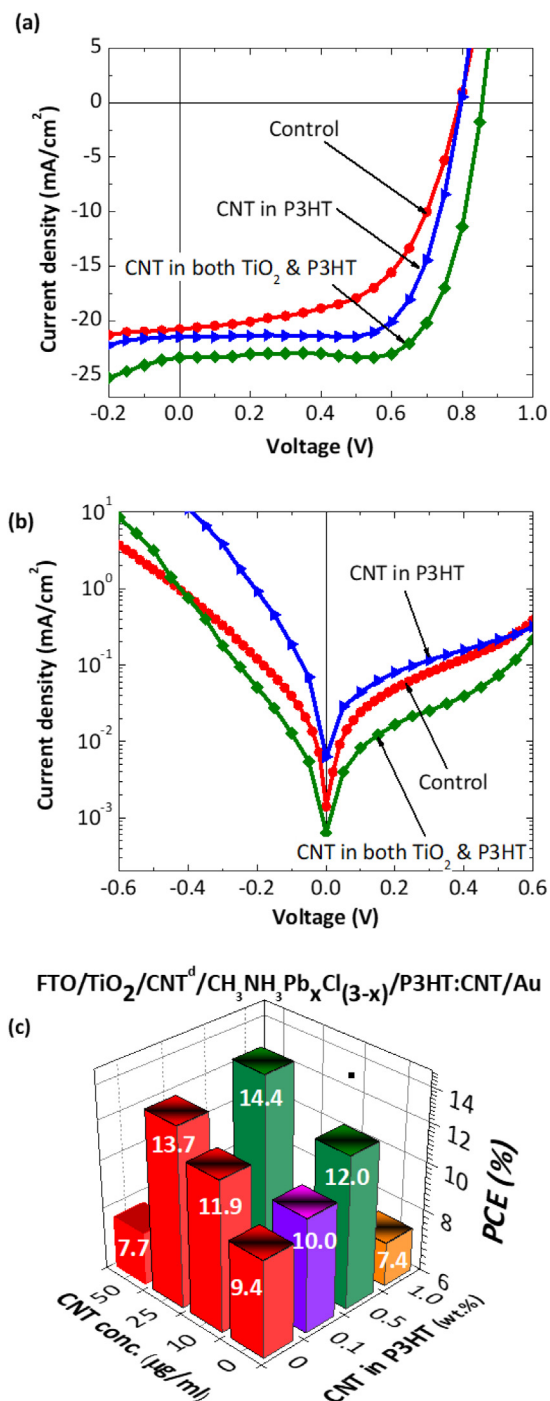


**Fig. 3.** (a) J-V characteristics of champion PSCs with and without CNT in TiO<sub>2</sub> and P3HT, having structure of FTO/TiO<sub>2</sub>/CH<sub>3</sub>NH<sub>3</sub>PbI<sub>x</sub>Cl<sub>3-x</sub>/P3HT/Au, (b) the corresponding semi-log J-V curves of the devices in dark, and (c) the PCE variation of the devices with CNT content.

is shown in Fig. 3(a) and their semi-log J-V curves in dark is shown in Fig. 3(b).

As shown in the Fig. 3(b), incorporation of CNT in the HTM increases the dark current, and, thus, indicates the improved hole-transport in the cell. The dark current is significantly suppressed when CNT was introduced at TiO<sub>2</sub>/CH<sub>3</sub>NH<sub>3</sub>PbI<sub>x</sub>Cl<sub>3-x</sub> interface and in P3HT which is an indication of increased recombination resistance. This could be due to reduced surface back-electron transfer at the TiO<sub>2</sub>/CH<sub>3</sub>NH<sub>3</sub>PbI<sub>x</sub>Cl<sub>3-x</sub> interface [15],

**Table 1**

The summary of the PV parameters of PSCs with and without CNT contents in TiO<sub>2</sub> and P3HT, respectively.

Device	J <sub>sc</sub> (mA/cm <sup>2</sup> )	V <sub>oc</sub> (V)	FF	PCE (%)
Control	19.09 ± 1.02	0.77 ± 0.01	0.53 ± 0.02	7.96 ± 0.76
CNT in TiO <sub>2</sub>	<b>20.86</b>	<b>0.79</b>	<b>0.57</b>	<b>9.35</b>
	20.86 ± 1.35	0.81 ± 0.03	0.68 ± 0.01	12.67 ± 0.43
CNT in P3HT	<b>22.85</b>	<b>0.85</b>	<b>0.70</b>	<b>13.67</b>
	19.36 ± 1.00	0.78 ± 0.02	0.68 ± 0.02	11.26 ± 0.69
CNT in both TiO <sub>2</sub> & P3HT	<b>21.53</b>	<b>0.80</b>	<b>0.70</b>	<b>12.07</b>
	21.47 ± 1.2	0.83 ± 0.02	0.69 ± 0.02	13.40 ± 0.41
	<b>23.52</b>	<b>0.86</b>	<b>0.71</b>	<b>14.37</b>

Parameters of the best cells are represented in bold.

which subsequently increased the V<sub>oc</sub> and fill-factor when tested under light.

Fig. 3(c) summarizes overall efficiencies of the devices with CNT at TiO<sub>2</sub>/CH<sub>3</sub>NH<sub>3</sub>PbI<sub>x</sub>Cl<sub>3-x</sub> interface and/or in P3HT, and the summary of the PV parameters are given in Table 1. The optimum device with CNT at both TiO<sub>2</sub>/perovskite interface and in P3HT showed power conversion efficiency of over 14%, which is over 50% enhancement when compared to control device without CNT incorporation. The enhancement is mainly due to increase in FF which is attributed to the increase in charge transport in CNT incorporated P3HT and surface passivation by CNT at TiO<sub>2</sub> / CH<sub>3</sub>NH<sub>3</sub>PbI<sub>x</sub>Cl<sub>3-x</sub>. Even though all PV parameters have been found to improve by varying degrees with the addition of CNTs, the major PV parameters responsible for the improved efficiencies are J<sub>sc</sub> and FF. This can be ascribed to the enhanced electron extraction and reduced charge recombination rates [12].

#### 4. Conclusion

In this work, the impact of the incorporation of CNT at TiO<sub>2</sub>/perovskite interface, in P3HT, and in both TiO<sub>2</sub>/perovskite interface and in P3HT has been studied. The best performance was achieved when CNT was incorporated in both TiO<sub>2</sub>/perovskite interface and P3HT, and above 50% enhancement in PCE was recorded compared to control device fabricated without incorporating CNT. Notably, all CNT incorporated PSCs exhibited higher FF, and it can be explained by the passivation of charge recombination.

#### Declaration of Competing Interest

The authors declare that they have no known competing financial interests or personal relationships that could have appeared to influence the work reported in this paper.

#### Acknowledgement

Authors acknowledge CBERC (LKA-3182-HRNCET), HRNCET (NORPART/2016/10237) projects and Ministry of Science Technology and Research, Sri Lanka for providing financial support.

#### Appendix A. Supplementary data

Supplementary data to this article can be found online at <https://doi.org/10.1016/j.matlet.2020.128174>.

## References

- [1] Z. Shi, A.H. Jayatissa, *Materials (Basel)* 11 (2018), <https://doi.org/10.3390/ma11050729>.
- [2] E.H. Jung, N.J. Jeon, E.Y. Park, C.S. Moon, T.J. Shin, T.Y. Yang, J.H. Noh, J. Seo, *Nature* 567 (2019) 511–515, <https://doi.org/10.1038/s41586-019-1036-3>.
- [3] M. Thambidurai, F. Shini, P.C. Harikesh, N. Mathews, C. Dang, J. Power Sources 448 (2020), <https://doi.org/10.1016/j.jpowsour.2019.227362> 227362.
- [4] J.A. Christians, R.C.M. Fung, P.V. Kamat, *J. Am. Chem. Soc.* 136 (2014) 758–764, <https://doi.org/10.1021/ja411014k>.
- [5] M. Batmunkh, T.J. Macdonald, C.J. Shearer, M. Bat-Erdene, Y. Wang, M.J. Biggs, I. P. Parkin, T. Nann, J.G. Shapter, *Adv. Sci.* 4 (2017) 1–11, <https://doi.org/10.1002/adv.201600504>.
- [6] S. Uthayaraj, D.G.B.C. Karunarathne, G.R.A. Kumara, T. Murugathas, S. Rasalingam, R.M.G. Rajapakse, P. Ravirajan, D. Velauthapillai, *Materials (Basel)* 12 (2019) 2037, <https://doi.org/10.3390/ma12132037>.
- [7] K. Balashangar, S. Paranthaman, M. Thanahaichelvan, P.A. Amalraj, D. Velauthapillai, P. Ravirajan, *Mater. Lett.* 219 (2018) 265–268, <https://doi.org/10.1016/j.matlet.2018.02.088>.
- [8] M. Thanahaichelvan, L.A. Browning, M.P. Dierkes, R.M. Reyes, A.V. Kralicek, C. Carraher, C.A. Marlow, N.O.V. Plank, *Data Br.* 21 (2018) 276–283, <https://doi.org/10.1016/j.dib.2018.09.093>.
- [9] M. Thanahaichelvan, L.A. Browning, M.P. Dierkes, R.M. Reyes, A.V. Kralicek, C. Carraher, C.A. Marlow, N.O.V. Plank, *Biosens. Bioelectron.* 130 (2019) 408–413, <https://doi.org/10.1016/j.bios.2018.09.021>.
- [10] G.J.H. Melvin, Q.Q. Ni, Y. Suzuki, T. Natsuki, *J. Mater. Sci.* 49 (2014) 5199–5207, <https://doi.org/10.1007/s10853-014-8229-9>.
- [11] T.J. Macdonald, M. Batmunkh, C.T. Lin, J. Kim, D.D. Tune, F. Ambroz, X. Li, S. Xu, C. Sol, I. Papakonstantinou, M.A. McLachlan, I.P. Parkin, J.G. Shapter, *J.R. Durrant, Small Methods* 3 (2019) 1–10, <https://doi.org/10.1002/smt.201900164>.
- [12] A.S.R. Bati, L.P. Yu, S.A. Tawfik, M.J.S. Spencer, P.E. Shaw, M. Batmunkh, *J.G. Shapter, IScience* 14 (2019) 100–112, <https://doi.org/10.1016/j.isci.2019.03.015>.
- [13] M. Cai, V.T. Tiong, T. Hreid, J. Bell, H. Wang, *J. Mater. Chem. A* 3 (2015) 2784–2793, <https://doi.org/10.1039/c4ta04997g>.
- [14] S. Ren, M. Bernardi, R.R. Lunt, V. Bulovic, J.C. Grossman, S. Gradečak, *Nano Lett.* 11 (2011) 5316–5321, <https://doi.org/10.1021/nl202796u>.
- [15] S.E.J. O’Kane, G. Richardson, A. Pockett, R.G. Niemann, J.M. Cave, N. Sakai, G.E. Eperon, H.J. Snaith, J.M. Foster, P.J. Cameron, A.B. Walker, *J. Mater. Chem. C* 5 (2017) 452–462, <https://doi.org/10.1039/c6tc04964h>.